

Aus dem Zentrum für Augenheilkunde der Universität zu Köln
Klinik und Poliklinik für Allgemeine Augenheilkunde
Direktor: Universitätsprofessor Dr. med. C. Cursiefen

Inflammatory and angiogenic response after full thickness transplantation of a fish scale–derived collagen matrix (FSCM)

Inaugural-Dissertation zur Erlangung der Doktorwürde
der Medizinischen Fakultät
der Universität zu Köln

vorgelegt von
Efthymios Alexandros Doulis
aus Athen, Griechenland

promoviert am 14. November 2022

Gedruckt mit Genehmigung der Medizinischen Fakultät der Universität zu Köln
Druckjahr 2023

Dekan:

Universitätsprofessor Dr. med. G. R. Fink

1. Gutachter:

Universitätsprofessor Dr. med. B. O. Bachmann

2. Gutachter:

Universitätsprofessor Dr. med. M.-E. Paulsson

ERKLÄRUNG

Ich erkläre hiermit, dass ich die vorliegende Dissertationsschrift ohne unzulässige Hilfe Dritter und ohne Benutzung anderer als der angegebenen Hilfsmittel angefertigt habe, die aus fremden Quellen direkt oder indirekt übernommenen Gedanken sind als solche kenntlich gemacht.

Bei der Auswahl und Auswertung des Materials sowie bei der Herstellung des Manuskriptes habe ich keine Unterstützungsleistungen erhalten.

Weitere Personen waren an der Erstellung der vorliegenden Arbeit nicht beteiligt. Insbesondere habe ich nicht die Hilfe einer Promotionsberaterin/eines Promotionsberaters in Anspruch genommen. Dritte haben von mir weder unmittelbar noch mittelbar geldwerte Leistungen für Arbeiten erhalten, die im Zusammenhang mit dem Inhalt der vorgelegten Dissertationsschrift stehen.

Die Dissertationsschrift wurde von mir bisher weder im Inland noch im Ausland in gleicher oder ähnlicher Form einer anderen Prüfungsbehörde vorgelegt.

Die in dieser Arbeit angegebenen Experimente sind nach entsprechender Anleitung durch Herrn Prof. Dr. med. Björn O. Bachmann, Herrn PD Dr. med. Dr. rer. nat. Deniz Hos und Herrn PD Dr. rer. nat. Felix Bock von mir selbst ausgeführt worden.

Die dieser Arbeit zugrunde liegenden Experimente sind von mir mit Unterstützung von Frau Dr. rer. nat. Maria Notara, Frau Dr. nat. med. Nasrin Refaian, Frau Dr. nat. med. Laura Schöllhorn, Frau PD Dr. med. Simona Schlereth und Herrn Mert Mestanoglu und den medizinisch-technischen Assistenten Herrn Tobias Braun und Frau Gabriel Braun durchgeführt worden.

Die Anästhesie und die Operationen an den Versuchstieren wurden von mir durchgeführt.

Erklärung zur guten wissenschaftlichen Praxis:

Ich erkläre hiermit, dass ich die Ordnung zur Sicherung guter wissenschaftlicher Praxis und zum Umgang mit wissenschaftlichem Fehlverhalten (Amtliche Mitteilung

der Universität zu Köln AM 132/2020) der Universität zu Köln gelesen habe und verpflichte mich hiermit, die dort genannten Vorgaben bei allen wissenschaftlichen Tätigkeiten zu beachten und umzusetzen.

Es wurde keine Forschung an Menschen durchgeführt.

Köln, den 22.01.2023

Efthymios Alexandros Doulis

X  _____

DANKSAGUNG

Die in dieser Arbeit angegebenen Experimente sind nach entsprechender Einarbeitung durch Herrn PD Dr. med. Dr. rer. nat. Deniz Hos und Herrn PD Dr. rer. nat. Felix Bock von mir selbst ausgeführt worden.

Die Ergebnisse der in dieser Arbeit gezeigten Experimente sind ausschließlich von mir nach Einarbeitung durch Herrn Prof. Dr. med. Björn O. Bachmann, Herrn PD Dr. med. Dr. rer. nat. Deniz Hos und Herrn PD Dr. rer. nat. Felix Bock selbstständig erarbeitet worden.

Die in-vitro Versuche, die Operationen an den Versuchstieren und die Auswertung der immunhistologischen Präparate wurden von mir persönlich durchgeführt.

TABLE OF CONTENTS

LIST OF ABBREVIATIONS.....	6
1. ABSTRACT	7
2. ZUSAMMENFASSUNG	9
3. INTRODUCTION	11
4. MATERIALS AND METHODS	14
4.1. Animals and anesthesia	14
4.2. Grafting of the FSCM	14
4.3. Cryosection tissue preparation and microscopy	15
4.4. In vitro scratch assay to demonstrate migration of lymphatic endothelial cells on FSCM17	
4.5. Data analysis and statistics	17
5. RESULTS.....	18
5.1. Histology and analysis of neovessel ingrowth and inflammatory invasion	18
5.2. Pachymetry and degradation	19
5.3. LEC migration assay	19
6. DISCUSSION	20
6.1. Conclusion	22
7. REFERENCES	25
8. APPENDIX	28
8.1. Figures.....	28
8.2. Tables	32

LIST OF ABBREVIATIONS

FSCM	Fish Scale-derived Collagen Membrane
MMP	Matrix Metalloproteinase
LEC	Lymphatic Endothelial Cells
WHO	World Health Organization
PBS	Phosphate-Buffered Saline
DAPI	4',6-Diamidino-2-Phenylindole
ROI	Region of Interest
IL-1	Interleukin-1
TNF- α	Tumor Necrosis Factor α

1. ABSTRACT

AIM OF THE STUDY: Corneal opacities are among the 5 leading causes of blindness worldwide. Due to a worldwide donor shortage of corneas, there is a high demand for alternative biomaterials for corneal transplantation. The aim of this study was to evaluate the short-term infiltration with inflammatory cells and corneal neovessels of a fish scale-derived collagen membrane (FSCM) as a corneal substitute in a murine normal risk corneal transplantation setting.

MATERIALS AND METHODS: Penetrating keratoplasty was performed in BALB/c recipient mice with the FSCM and allogenic corneal transplants from C57BL/6 mice as controls. The transplanted FSCMs/allogenic corneas were removed after two weeks. Cryosections were stained immunohistologically for inflammatory cells and corneal blood and lymphatic vessels using F4/80, CD11b, CD45, CD31 and Lyve1. Inflammatory cells, hemangiogenesis and lymphangiogenesis were analyzed and quantified morphometrically by using a semiautomatic method based on the image analyzing program Cell[^]F. To analyze the degradation of the FSCM, thickness measurements were performed, with non-implanted FSCMs as control group.

In vitro, FSCM-coated wells (and uncoated wells as controls) were incubated for 24 hours with lymphatic endothelial cells (LECs) and a cell migration (scratch assay) was performed to analyze the migratory capacity of LECs on the FSCM surface.

RESULTS: The FSCMs showed neither neovascular nor inflammatory invasion when compared to allogenic transplants (mean percentage of antibody-positive area in transplant: for CD31: FSCM: 0%, controls: 2.8%, $p=0.098$; for Lyve1: FSCM: 0%, controls: 1.9%, $p=0.049$; for F4/80: FSCM: 0%, controls: 10.4%, $p=0.0067$; for CD45: FSCM: 0%, controls: 41.8%, $p=0.0098$; for CD11b: FSCM: 0%, controls: 24.0%, $p=0.016$).

Thickness measurements of the implanted FSCMs showed variable but on average no thinning as a possible sign for degradation when comparing to the control group (average minimal thickness of implanted FSCM: 38.24 μm , controls: 21.35 μm , $p=0.060$).

The migratory capacity of LECs was similar on FSCM-coated and uncoated wells (mean percentage of LEC-free area at 6 h post scratch: FSCM: 77.6%, controls: 83.1%,

p=0.488; at 12 h post scratch: FSCM: 59.5%, controls: 63.8%, p=0.717; at 24 h post scratch: FSCM: 9.0%, controls: 9.8%, p=0.859). LECs on the FSCM migrated along its surface ridges and showed no signs of invasion into the FSCM matrix.

CONCLUSIONS: Our results indicate that the FSCM resists short-term inflammatory and neovessel infiltration, which suggests a reduced risk for postoperative immune reaction. Incubation for two weeks in the murine cornea did not cause any significant degradation. This study warrants further investigation on its short- and long- term effects and its potential use as donor substitute in keratoplasty.

2. ZUSAMMENFASSUNG

ZIEL DER STUDIE: Hornhauttrübungen gehören weltweit zu den Top 5 Ursachen von Blindheit. Aufgrund des weltweiten Mangels an Hornhautspendern besteht ein großer Bedarf nach alternativen Biomaterialien für Hornhauttransplantationen. Ziel dieser Arbeit war, die entzündliche Reaktion nach Implantation einer aus Fischeschuppen gewonnenen Kollagenmembran (FSCM) als Ersatz für Spenderhornhäute im Rahmen einer Normalrisiko-Keratoplastik bei Mäusen zu charakterisieren.

MATERIALIEN UND METHODEN: Transplantationen in die Hornhaut wurden bei BALB/c-Empfängermäusen mit der FSCM und mit allogenen Hornhauttransplantaten von C57BL/6-Mäusen als Kontrolle durchgeführt. Die transplantierten FSCMs/allogenen Hornhäute wurden nach zwei Wochen entfernt. Die Kryoschnitte wurden immunhistologisch auf Entzündungszellen und Blut- und Lymphgefäße in der Hornhaut mit F4/80, CD11b, CD45, CD31 und Lyve1 angefärbt. Entzündungszellen, Hämangiogenese und Lymphangiogenese wurden mit Hilfe eines halbautomatischen Verfahrens, das auf dem Bildanalyseprogramm Cell[^]F basiert, morphometrisch analysiert und quantifiziert. Um die Degradation der FSCM zu analysieren, wurden Dickenmessungen durchgeführt, wobei nicht implantierte FSCM als Kontrollgruppe analog zu den transplantierten Membranen prozessiert wurden.

In vitro wurden FSCM-beschichtete Wells (und unbeschichtete Wells als Kontrollen) 24 Stunden lang mit lymphatischen Endothelzellen (LECs) kultiviert. Danach wurde eine Zellmigrationsanalyse (Scratch-Assay) durchgeführt, um die Migrationsfähigkeit der LECs auf der FSCM-Oberfläche zu analysieren.

ERGEBNISSE: Die FSCM zeigten im Vergleich zu allogenen Transplantaten keine neovaskuläre oder entzündliche Invasion (mittlerer Prozentsatz der Antikörper-positiven Fläche im Transplantat: für CD31: FSCM: 0%, Kontrollen: 2,8%, $p=0,098$; für Lyve1: FSCM: 0%, Kontrollen: 1,9%, $p=0,049$; für F4/80: FSCM: 0%, Kontrollen: 10,4 %, $p=0,0067$; für CD45: FSCM: 0 %, Kontrollen: 41,8%, $p=0,0098$; für CD11b: FSCM: 0%, Kontrollen: 24,0%, $p=0,016$).

Dickenmessungen der implantierten FSCM zeigten keine signifikante Degradierung im Vergleich mit der Kontrollgruppe, wobei die Dickenmessungen nach Implantation

deutliche interindividuelle Schwankungen zeigten (durchschnittliche minimale Dicke der implantierten FSCM: 38,24 μm , Kontrollen: 21,35 μm , $p=0,060$).

Die Migrationsfähigkeit der LECs war auf FSCMs und den Kulturplatten (Kontrollen) vergleichbar (mittlerer Prozentsatz der LEC-freien Fläche 6 Stunden nach dem Ritzen: FSCM: 77,6%, Kontrollen: 83,1%, $p=0,488$; 12 Stunden nach dem Ritzen: FSCM: 59,5%, Kontrollen: 63,8%, $p=0,717$; 24 Stunden nach dem Ritzen: FSCM: 9,0%, Kontrollen: 9,8%, $p=0,859$). LECs auf der FSCM migrierten entlang der Oberflächenrippen und zeigten keine Anzeichen einer Invasion in die FSCM-Matrix.

SCHLUSSFOLGERUNGEN: Unsere Ergebnisse deuten darauf hin, dass die FSCM einer kurzfristigen entzündlichen und neovaskulären Infiltration widersteht, was auf ein geringeres Risiko für postoperative Immunreaktionen schließen lässt. Die zweiwöchige Inkubation in der Hornhaut von Mäusen führte zu keiner signifikanten Degradation. Diese Studie rechtfertigt weitere Untersuchungen zu den kurz- und langfristigen Auswirkungen der FSCM und ihrer möglichen Verwendung als Spenderersatz bei Keratoplastiken.

3. INTRODUCTION

The cornea is the clear “window” to the eye, serves as the primary front barrier of the eye against trauma and infection, and contributes, with ~43 dpt to ~70% of its refractive power. It consists of different layers (from anterior to posterior): a multi-layered epithelium which undergoes constant mitosis, the Bowman layer, a tough stroma consisting of collagen fibrils, Descemet’s membrane, and a single-layered endothelium ¹. It has rich innervation that is provided by the trigeminal nerve. The cornea is a transparent, avascular tissue and is supplied through diffusion of nutrients from the tear film, the aqueous of the anterior chamber of the eye and the corneal limbus ². This angiogenic privilege of the cornea is critical to its transparency by preventing vessel growth in it ³⁻⁵. To stay free of opacities, all corneal layers are being constantly dehydrated by specialized corneal endothelial cells ¹.

The response to trauma differs for the three main layers of the cornea. Breaks to the epithelial barrier are directly tended to by the neighbouring cells through cell migration and cell spreading, at a rate of 60 to 80 mm per hour. 24 to 30 hours after injury, mitosis restores the epithelial cell population. In the case of stromal injury, the wound healing process resembles the cutaneous one, albeit without the presence of vessels. Stromal keratocytes are activated and take on the appearance of fibroblasts. Later processes involve myofibroblasts expressing matrix metalloproteinases (MMPs) and activating cytokines to rearrange stromal collagen fibrils. Finally, endothelial cells are not known to undergo *in vivo* mitosis. Areas of damaged endothelial cells are covered by migration and enlargement of neighbouring cells ⁶.

Corneal opacification is the loss of normal transparency of the cornea. Corneal transparency depends on the uniformity and regularity of the arrangement of collagen within the corneal stroma. Alterations in this arrangement, for example in the cases of trauma, ulceration, edema, infection or genetic diseases, is manifested as corneal opacity.

According to the World Health Organization (WHO), 4,2 million people suffer from vision impairment or blindness due to corneal opacities ⁷. Many of these patients could be helped by corneal transplantation but, in stark contrast, only about 100.000 corneas

are transplanted each year. This is mostly due to a lack of donor corneas and that, in patients with increased risk of rejection or wound healing problems, transplantation with normal grafts is often not attempted.

Xenotransplantation, the transplantation of tissue from other species (e.g. primates, pigs, cows, sheep, dogs, fish) has been extensively tested as an alternative to human tissue transplantation, but grafts from most donor species result in graft rejection ⁸.

Biosynthetic hypo- or acellular artificial grafts could offer a viable alternative to human corneal grafts to bridge the current availability gap. A clinical study from Fagerholm *et al.* in 2010 showed promising results of keratoplasties using a biosynthetic graft consisting of recombined human type I collagen ⁹. However, the biosynthesis of corneal extracellular matrices tends to be complicated and costly ¹⁰⁻¹². A fish scale-derived collagen matrix (FSCM) (BioCornea, Aeon Astron B.V., Leiden, Netherlands), an acellular matrix consisting of type I collagen, is currently being tested in multiple international centers (COST BM 1302). The largest part of the matrix consists of collagen fibers with a parallel structure, similar to the human corneal stroma and a reticular surface, similar to the human Bowman-layer. It is derived from the decellularized, decontaminated and decalcified scale of the Mozambique tilapia (*Oreochromis mossambicus*) and is therefore cost-efficient and widely available. Lin *et al.* ¹³, who developed the production technique, showed in 2010 that corneal epithelial cells can adhere on the FSCM's surface and will proliferate and migrate, primarily along its natural ridges. It can therefore be used as a carrier for corneal epithelial cells and, due to its high light- and oxygen-permeability, might be a good candidate as a biosynthetic corneal graft ¹².

It is evident that an analysis of the postoperative invasion of an implanted FSCM through neovessels and inflammatory cells is of great importance in its evaluation as a viable candidate for transplantation as a corneal biosynthetic xenograft. Yuan *et al.* performed in their study ¹⁴ pocket implantations of FSCMs in the corneal stroma of rabbits. The rabbits showed clinically no corneal haze or ulcers in the area of implantation, even 6 months after surgery, hinting at low rejection risk. Van Essen *et al.* ¹⁵ evaluated the invasion of FSCMs by neovessels and inflammatory cells after lamellar transplantation in rat corneas. They found mild to moderate infiltration of leukocytes of the surrounding tissue and few inflammatory cells within FSCMs. Hos

et al. demonstrated in a murine full thickness keratoplasty model less blood- and lymphatic neovascularization in the area of the implanted FSCM compared to the control group (penetrating keratoplasty with allogeneic full thickness murine corneal grafts) by analysis of wholemount preparations.¹⁶

Until now most analyses of corneal biocompatibility of FSCM have been performed in non-penetrating grafting experiments. We wanted to analyze potential short-term biodegradation in a murine model where FSCMs are used as full thickness grafts for penetrating keratoplasty, where the post-implantation inflammatory reaction is, in theory, more intense. The aim of this study was to further analyze the amenability of the FSCM and the surrounding corneal tissue to short-term neoangiogenic and inflammatory invasion after penetrating keratoplasty. Since the formation of lymphatic vessels in corneal transplants is an important factor for the initiation of immune reactions and for wound healing, we wanted to analyze migratory patterns and the migration speed of human lymphatic endothelial cells (LEC) on the surface of the FSCM.

4. MATERIALS AND METHODS

4.1. Animals and anesthesia

The *in vivo* experiments were conducted in accordance with the Association for Research in Vision and Ophthalmology's Statement for the Use of Animals in Ophthalmology and Vision Research and institutional guidelines regarding animal experimentation. The animal experimentation contract number for this study was TVA 84-02.04.2013.A066.

Full thickness transplantation into the corneas of 6-8 weeks old female BALB/C mice was performed either with FSCM or with corneas of 6-8-week-old C57BL/6J as controls. For all surgical procedures mice were deeply anesthetized with an intraperitoneal injection of Ketanest® S (PFIZER PHARMA PFE GmbH, Berlin, Germany, Ketamine 8 mg/kg) and Rompun® (Bayer Vital GmbH Geschäftsbereich Pharma, Leverkusen, Germany, Xylazine 0.1 ml/kg).

4.2. Grafting of the FSCM

Circular grafts were prepared from either 40 µm thick FSCMs or from corneas from freshly euthanized C57BL/6J mice (control group) using a 1,5 mm diameter trephine (Kai Standard Biopsy Punch, Seki, Gifu Prefecture, Japan). A penetrating transplantation was performed on the right eye of BALB/C mice. The central cornea of each mouse was excised using a same-sized trephine. Afterwards, the graft was implanted in the host cornea using 8 11-0 nylon sutures (Serag Wiessner, Naila, Germany). Sutures were left in place for the duration of the experiment. At the end of the surgery the eyes were covered with Floxal® antibiotic eye ointment (BAUSCH & LOMB, Schiphol-Rijk, Germany, Ofloxacin 3 mg/g) and a complete tarsorrhaphy was performed to protect the eye postoperatively, using three 8-0 nylon sutures (Serag Wiessner, Naila, Germany).

Sutures were left in place for the duration of the experiment. The tarsorrhaphies dissolved spontaneously in the course of the first 5 postoperative days in all mice. Regular clinical check-ups were performed. Floxal® antibiotic eye ointment

(BAUSCH & LOMB, Schiphol-Rijk, Germany, Ofloxacin 3 mg/g) was administered to the operated eye once daily for the remainder of the experiment. All BALB/C mice were euthanized by CO₂ inhalation after 2 weeks and the eyes were removed for further analysis.

4.3. Cryosection tissue preparation and microscopy

To analyze the short-term neovascular and inflammatory invasion of the implanted FSCM, we used immunohistochemical markers on central cryosections of treatment and control corneas, to trace the path of the neovessels and the position of the inflammatory cells in relation to the graft.

Obtained samples were cut using a Cryostat-microtome at -20 °C (LEICA CM3050 S, Leica Microsystems, Wetzlar, Germany) and mounted on microscope slides. The slides were then dried for 15 minutes at room temperature. The samples were afterwards fixed in acetone for 15 minutes and subsequently washed 3 times for 5 minutes in PBS (Phosphate-buffered saline, powder pack, PanReac AppliChem, Darmstadt, Germany). They were then Fc-blocked using a 2% BSA solution in PBS for 60 minutes in a slide incubation chamber (M922 – StainTray™ 30 slides staining system, Simport Scientific, Bernard-Pilon Beloeil, Quebec, Canada). The following primary antibodies were used:

F4/80 (uncoupled) rat anti-mouse in a PBS solution of 1:300 (Thermo Fisher Scientific GmbH, Dreieich, Germany)

CD11b FITC rat anti-mouse in a PBS solution of 1:200 (Bio-Rad AbD Serotec GmbH, Puchheim, Germany)

CD45 (uncoupled) rat anti-mouse in a PBS solution of 1:200 (Abcam plc, Cambridge, United Kingdom)

Lyve1 (uncoupled) rabbit anti-mouse in a PBS solution of 1:500 (AngioBio, San Diego, CA, United States)

CD31 FITC rat anti-mouse in a PBS solution of 1:400 (BD Biosciences Pharmingen, CA, United States)

Antibodies were left overnight at 4 °C. The next day, slides were washed 3 times for 5 minutes in PBS. For unconjugated primary antibodies goat anti-rat Alexa 555 in a

PBS solution of 1:250 (Sigma-Aldrich, Taufkirchen, Germany) or goat anti-rabbit Cy3 in a PBS solution of 1:500 (dianova GmbH, Hamburg, Germany) secondary antibodies were left on the slides for 45 minutes at room temperature. Afterwards, the slides were washed 3 times for 5 minutes in PBS and left in a DAPI solution in PBS of 1:1000 for 5 minutes in the dark at room temperature. Finally, the slides were washed 3 times for 5 minutes and sealed with DAKO fluorescent mounting medium (Abcam plc, Cambridge, United Kingdom).

The samples were photographed with a Primo Vert inverted microscope (ZEISS, Oberkochen, Germany) microscope mounted with a XM10 camera (Olympus, Tokyo, Japan) and analyzed morphometrically by using a semiautomatic method based on the image analyzing program Cell[^]F (Olympus, Tokyo, Japan). Only slides from central slices of the cornea were analyzed. Two series of analyses were performed, depending on the region of interest (ROI) being analyzed. In the first analysis, the objective was to analyze the neovascular and inflammatory invasion of the FSCM. The region of interest for the FSCM group consisted of the transplanted FSCM, whereas for the control group, the region of interest consisted of the transplanted cornea. In the second analysis, the objective was to analyze the neovascular and inflammatory reaction of the recipient corneal tissue, of which the ROIs consisted.

To evaluate the level of degradation of the implanted FSCM between the time of implantation and excision, the thinnest point of the FSCM in each of the samples was measured by means of the image analyzing program Cell[^]F. As control for the degradation-evaluation thickness measurement, five of the same 40 µm thick FSCMs were cut using a Cryostat-microtome at -20 °C and mounted on microscope slides. The slides were then again dried for 15 minutes at room temperature. The samples were fixed in acetone for 15 minutes and subsequently washed 3 times for 5 minutes in PBS. This constituted a replication of the histological preparation-procedure for the incubated group of FSCMs, in order to replicate the same settings for optimal data quality. The thinnest point of the FSCM in each of the samples was again measured by means of the image analyzing program Cell[^]F.

4.4. In vitro scratch assay to demonstrate migration of lymphatic endothelial cells on FSCM

To determine whether lymphatic endothelial cells (LECs) migrate on the FSCMs a scratch assay was performed. FSCM discs of 40 μm thickness were placed at the bottom of 4 wells of a 24-well plate. The FSCMs were immobilized on the t/c plastic of the wells using 30G needles. 4 wells without FSCM served as control. LECs were seeded at a concentration of 6×10^4 cells/well in endothelial cell medium overnight in each well. The medium was replaced by endothelial cell medium supplemented with 0.5 mM hydroxyurea (Sigma-Aldrich, Taufkirchen, Germany) to arrest cell growth and incubated for a further 24 hours. A scratch was made using a sterile 200- μL pipette tip (Eppendorf, Hamburg, Germany) which resulted in a uniform and standardized distance between the wound edges of the cell-free scratch. Cells were washed twice with PBS, and equal volumes of endothelial cell medium were added. The scratch area was then photographically documented at various time points over 30 hours. The analysis of the pictures was performed by ImageJ software (ImageJ 1.48v; <http://imagej.nih.gov/ij/>; provided in the public domain by the National Institutes of Health, Bethesda, MD, USA).

4.5. Data analysis and statistics

Data for the animal trials was analyzed and collected with the image analyzing program Cell[^]F. For the in vitro assay data, the image analyzing program ImageJ was used.

Unless otherwise stated, group measures are given as mean \pm standard deviation (SD).

Statistical analysis was performed using the software Microsoft Excel (Microsoft, Redmond, Washington, United States).

Data and respective controls were compared with a student's t-test. All tests were unpaired and two-tailed, with significance accepted at $P < 0.05$.

5. RESULTS

5.1. Histology and analysis of neovessel ingrowth and inflammatory invasion

In the *in vivo* experiment, of the five transplanted FSCMs, three resulted in partial epithelialization in the two-week timeframe after implantation, whereas the remaining two showed little to no epithelialization and were excluded from the data analysis, since the implantation could not be considered successful. The reason for the lack of epithelialization could not be identified, although a significance in level difference between host cornea- and implanted FSCM-interface was suspected.

All mice showed varying levels of secondary cataracts postoperatively. None showed any signs of infection or postoperative haze. The FSCM showed zero ingrowth of blood- and lymphatic neovessels and no invasion with inflammatory cells (0% antibody-positive area percentage in the FSCM). In the control group, the average of the antibody-positive area percentage inside the transplanted corneal stroma for the applied biomarkers was: for CD31 2.8%, for Lyve1 1.9%, for F4/80 10.4%, for CD45 41.8% and for CD11b 24.0%. For the applied biomarkers CD31, Lyve1, F4/80, CD45 and CD11b, the respective p-values for the analyses were 0.098, 0.049, 0.007, 0.01 and 0.016. Assuming that a p-value less or equal to 0.05 indicates statistically significant results, analysis with all applied markers excluding CD31 showed statistically significant results. Immunohistochemistry showed complete imperviousness of the FSCM collagen matrix to neovascular ingrowth and inflammatory invasion, which confirmed previous findings.^{16 15,17}

In the analysis of the neovascular and inflammatory reaction in the recipient tissue of both groups, the average of the antibody-positive area percentage for the FSCM group for the applied biomarkers was: for CD31 3.82%, for Lyve1 2.42%, for F4/80 19.92%, for CD45 24.21% and for CD11b 24.82%. For the control group, the average of antibody-positive area for the applied biomarkers was: for CD31 3.8%, for Lyve1 2.49%, for F4/80 10%, for CD45 18.88% and for CD11b 31.92%. For the applied biomarkers CD31, Lyve1, F4/80, CD45 and CD11b, the respective p-values for the

analyses were 0.99, 0.895, 0.464, 0.696 and 0.714. This analysis didn't produce statistically significant results.

5.2. Pachymetry and degradation

The thickness of the implanted FSCM at the moment of excision (2 weeks postoperatively) was measured to have an average of 38.2 μm , with a standard deviation of 17.3 μm (original FSCM thickness was 40 μm). The control group's FSCM thickness after the same histological preparation was measured to have an average of 21.4 μm , with a standard deviation of 2.9 μm . The p-value for the analysis was 0.06, indicating a not-statistically significant difference between the two groups. In the sections where there was thickening of the FSCM, empty (possibly fluid-filled) caverns were observed between its fibers, hinting to an artifact resulting from the preparation technique or, alternatively, a form of degradation of the FSCM. Similarly, in the sections where the FSCM was at its thinnest, a chipping of its fibres could be observed.

5.3. LEC migration assay

In the in vitro experiment, the LEC migration speed in the FSCM-coated wells showed no significant difference to the bare, t/c plastic control group at any of the different measured time points (after 6 hours: FSCM cell-free area average=77.61%, control cell-free area average=83.1%, FSCM STDV=11.42, control STDV=8.13, t-test $p=0.488$, after 12 h: FSCM cell-free area average=59.52%, control cell-free area average=63.83%, FSCM STDV=22.42, control STDV=5.18, t-test $p=0.717$, after 24 hours: FSCM cell-free area average=9.04%, control cell-free area average=9.8%, FSCM STDV=3.34, control STDV=6.1, t-test $p=0.859$). Assuming that a p-value less than 0.05 indicates statistically significant results, results of the migration assay were not statistically significant. The LECs migrated mainly along the natural ridges of the FSCM's surface.

6. DISCUSSION

Our goals with the *in vivo* experiments were to further test the use of FSCM as a replacement therapy for corneal stroma, to study its short-term immunogenicity and neovascularization after implantation and to study its *in situ* degradation (or possible lack thereof).

Most of the penetrating keratoplasties we performed with the FSCM resulted in partial epithelialization after two weeks. This confirms results of other studies; Hos *et al.*¹⁶ penetrating keratoplasties also resulted in epithelialization of the implanted FSCM, while van Essen *et al.*^{15,17} showed that human corneal epithelial cells can grow on the FSCM surface. No eye showed complete epithelialization; two mice showed a complete lack thereof. Although the reason for this remains unclear, we suspected a significant level difference between host cornea- and implanted FSCM-interface, so that the corneal epithelial cells couldn't "climb" to the anterior FSCM-surface. Optimizing the graft thickness and the surgical technique could allow to assess the *in vivo* capacity of FSCM for epithelialization in a murine model. Another reason for the poor epithelialization could be mechanical: after the tarsorrhaphies were dissolved (minimum timepoint third postoperative day, maximum timepoint fifth postoperative day), mice were observed to rub their ocular region (possibly due to foreign-body sensation). The possibility of a cytotoxic reaction of the corneal epithelium to the implanted FSCM is low; van Essen *et al.* study¹⁷ showed that the FSCM had no cytotoxic effects on human corneal epithelial and stromal cells. Van Essen *et al.*'s study also showed adequate adhesion of human corneal epithelium cells on the matrix; it is therefore unlikely that a lack of adhesive support of FSCMs for epithelial cells was the reason for the low epithelialization rate.

Lyve1 and CD31 markers were used to detect lymphatic and blood endothelial cells respectively. CD45 is a marker for all leukocytes, F4/80 detects macrophages, while CD11b is used as a marker for neutrophilic granulocytes, monocytes and memory B cells¹⁸. The implanted FSCMs showed no invasion of the immunohistochemically traced neovessels and inflammatory cells. There was neovascularization surrounding

the FSCM, which was also observed in previous studies ^{3,4,15-17}. Inflammatory cells of all three traced markers were detected on the margins of the FSCM and in high concentrations in the area surrounding sutures, indicating that a large percentage of the inflammation was caused by irritation from sutures. There was no statistically significant difference in the marker-positive area in the recipient corneas for the FSCM and the control group. This suggests that the reactivity of an implanted FSCM is not significantly different to that of an implanted allogeneic corneal graft. Our results further hint that the FSCM possesses low short-term immunogenicity, which would make it ideal as a corneal stroma replacement therapy for corneal perforations during the acute, high-risk phase. The reason for this impermeability of the FSCM to neovessels and inflammation cells is believed to be the tight structure of its collagen fibers. Future research on its applications, even as a long-term solution for corneal stroma substitution should be considered. Fagerholm *et al.* ¹⁹ used a biosynthetic graft consisting of recombined human type I collagen implanted in humans, a material that is most similar to the FSCM in comparison to other materials being tested right now, and showed stable results up to four years of follow-up in ten patients, although it resulted in corneal thinning. Van Essen *et al.* in their 2013 study ¹⁵ suspected higher amounts of light scatter from the FSCM in comparison to the normal human cornea, something that can theoretically be optimized with removal of the micropattern.

The FSCMs showed variable thickness at the two-week timepoint after implantation (stable thickness, thickening and thinning were observed in different mice and parts of the FSCM). The thickened FSCM showed empty (possibly fluid-filled) caverns between its fibers. This could be a result of interaction with the host corneal tissue or a result of the preparation method of the cryosection slides. The thinner FSCM could also be an artifact of the cryosection preparation method and subsequent microscopy. Alternatively, it could be a hint for degradation. F4/80 positive staining (hinting the presence of macrophages) was detected at the margins of all implanted FSCMs. This, however, is in stark contrast to previous results ¹⁷, where intrastromally implanted FSCMs in rabbits showed stable thickness six weeks after implantation. Another explanation for this could be the different implantation technique: penetrating keratoplasty with intrastromal suturing of FSCMs could in theory, being more

invasive, cause a more intense inflammatory reaction compared to intrastromal implantation. The fact that the non-implanted FSCMs in the control group showed no statistically significant difference to the implanted FSCMs indicates that at least part of this degradation is in fact due to the histological preparation of the membranes, since the control group lacked any incubation time in a murine cornea.

Our goals with the scratch assay were to observe the migrating pattern of LECs (an important component of lymphatic neovascularization) on the FSCM and to determine the speed of LEC migration. The scratch assay showed that LECs can migrate on the FSCM surface. It also indicates that LECs have a similar migration speed on the FSCM surface compared to the bare well plate plastic. The LECs migrated along the natural ridges of the FSCM surface, supporting the previous findings^{13,17} and indicating that the micropattern dictates the trajectory of cell migration. LECs migrating on the FSCM surfaces would mean that neovascularization anteriorly or posteriorly is possible, even though it resists invasion into the biomaterial. A neovascularization of this level could imply a higher risk for immune reactions/rejection and, if it reaches the visual axis, it would also lower visual acuity²⁰.

6.1. Conclusion

Our results support existing data showing that FSCMs could be a future short-term replacement therapy for human corneal stroma, e.g. in emergency cases, such as larger corneal perforations. It shows low immunogenicity, which is optimal for its use as a graft. Its production method is, in comparison to similar existing materials on the market, cheap and efficient and the source for its basic materials is, in stark contrast to the current deficit of human corneal grafts, abundant. Further, longer-term research should focus on the optimization of its properties and suturing and on its long-term immunogenicity and biocompatibility^{11,21}.

Since the human corneal endothelium has no regeneration ability, it is as-of-yet not considered as a possible graft solution for patients needing a full-thickness or endothelial keratoplasty, although its application in an anterior lamellar keratoplasty

is yet to be tested ²². Yet, it is unclear whether an endothelial layer is even necessary in these grafts to maintain optical clarity.

The FSCM does, however, show promising results as a tectonic tamponade-solution in cases of corneal perforation. It was shown that the FSCM can be used successfully to treat larger corneal perforations in a pig model²³. Furthermore, in a rat and in a mouse model respectively, it was shown that a stromally sutured FSCM in penetrating keratoplasty can be epithelialized from the recipient's epithelial cells ^{15,16}. In addition, subcutaneously implanted FSCMs in rats and intrastromally implanted FSCMs in rabbits exhibit hardly any infiltrating immune cells¹⁷.

Corneal perforations represent an ophthalmological emergency due to their devastating consequences, such as infection, corneal scarring and secondary glaucoma and cataract. Emergency medical and surgical treatment to restore the anatomical integrity of the globe, salvage visual function as much as possible and reduce the probability of complications to a minimum is mandatory ^{24,25}. The underlying conditions or disorders responsible for corneal ulcerations, and subsequently for corneal perforations, are numerous, and can be either isolated or superimposed ²⁶.

The choice of the treatment can be influenced by various factors: size, depth and location of the perforation, etiology of the perforation and immune status of the patient. In cases of smaller corneal defects, tissue adhesives, amniotic membrane transplantation, conjunctival flap or patch grafts can be used. In cases of failure of previous treatments or larger, more than three millimeter in diameter, perforations, high-risk penetrating or lamellar emergency keratoplasty should be considered ^{27,28}. Previous studies have shown that high-risk keratoplasties have a higher occurrence of rejection-related graft failure resulting in postoperative corneal opacities ²⁹ and can have an up to 70% rejection rate despite intense local immunosuppressive therapy ³⁰⁻³³. Although lamellar keratoplasty has augmented graft survival rate even in cases of high-risk corneas, immunological reasons are still the most common cause of graft failure ^{34,35}. The reason for this is the intense inflammatory reaction that accompanies the acute phase of most cases of corneal perforation. A high-risk cornea, e.g. a recently perforated cornea, often exhibits vascularization of the cornea, increased lymphatic drainage to cervical lymph nodes, corneal migration of leukocytes, maturation of local epithelial leukocytes and stromal dendritic cells, and increase of pro-inflammatory

cytokines, such as interleukin-1 (IL-1) and tumor necrosis factor α (TNF- α)³⁶⁻³⁹. The corneal immune privilege can thus be disturbed in a high-risk cornea, leading to a higher likelihood for short-term immune reaction and rejection of a possible graft⁴⁰⁻⁴⁷. This supports the need for a tectonic tamponade solution in high-risk, perforated corneas with larger defects, optimally one that exhibits a lower tendency to neovascularization and inflammation, to bridge this short-term, high-risk phase, until a keratoplasty can later be performed, without wasting a corneal graft⁴⁸. A penetrating keratoplasty with a FSCM in cases of bigger perforations could potentially solve the problem of the temporary tamponade for the highly inflammatory phase, until an allogeneic corneal transplantation at a later time point can be achieved^{14,49}. It could also solve the problem of reduced availability of corneal tissue and the lack of eye banking facilities in many parts of the world^{24,50}.

7. REFERENCES

1. DelMonte DW, Kim T. Anatomy and physiology of the cornea. *J Cataract Refract Surg* 2011; **37**(3): 588-98.
2. Cursiefen C. Immune privilege and angiogenic privilege of the cornea. *Chem Immunol Allergy* 2007; **92**: 50-7.
3. Cursiefen C, Chen L, Dana MR, Streilein JW. Corneal lymphangiogenesis: evidence, mechanisms, and implications for corneal transplant immunology. *Cornea* 2003; **22**(3): 273-81.
4. Hadrian K, Willenborg S, Bock F, Cursiefen C, Eming SA, Hos D. Macrophage-Mediated Tissue Vascularization: Similarities and Differences Between Cornea and Skin. *Front Immunol* 2021; **12**: 667830.
5. Clahsen T, Buttner C, Hatami N, Reis A, Cursiefen C. Role of Endogenous Regulators of Hem- And Lymphangiogenesis in Corneal Transplantation. *J Clin Med* 2020; **9**(2).
6. Bukowiecki A, Hos D, Cursiefen C, Eming SA. Wound-Healing Studies in Cornea and Skin: Parallels, Differences and Opportunities. *Int J Mol Sci* 2017; **18**(6).
7. Bourne RRA, Flaxman SR, Braithwaite T, et al. Magnitude, temporal trends, and projections of the global prevalence of blindness and distance and near vision impairment: a systematic review and meta-analysis. *Lancet Glob Health* 2017; **5**(9): e888-e97.
8. Hara H, Cooper DK. Xenotransplantation--the future of corneal transplantation? *Cornea* 2011; **30**(4): 371-8.
9. Fagerholm P, Lagali NS, Merrett K, et al. A biosynthetic alternative to human donor tissue for inducing corneal regeneration: 24-month follow-up of a phase 1 clinical study. *Sci Transl Med* 2010; **2**(46): 46ra61.
10. Schrage N, Hille K, Cursiefen C. [Current treatment options with artificial corneas: Boston Kpro, Osteo-odontokeratoprosthesis, Miro Cornea(R) and KeraKlear(R)]. *Ophthalmologe* 2014; **111**(11): 1010-8.
11. Schaub F, Matthaei M, Enders P, et al. [Treatment of vascularized high-risk eyes with a Boston keratoprosthesis]. *Ophthalmologe* 2021; **118**(6): 544-52.
12. Bachmann BO, Schrader S. [Biomaterials or Donor Tissue - What is the Future of Tissue Engineering for Cornea Reconstruction?]. *Klin Monbl Augenheilkd* 2017; **234**(6): 758-62.
13. Lin CC, Ritch R, Lin SM, et al. A new fish scale-derived scaffold for corneal regeneration. *Eur Cell Mater* 2010; **19**: 50-7.
14. Yuan F, Wang L, Lin CC, Chou CH, Li L. A cornea substitute derived from fish scale: 6-month followup on rabbit model. *J Ophthalmol* 2014; **2014**: 914542.
15. van Essen TH, Lin CC, Hussain AK, et al. A fish scale-derived collagen matrix as artificial cornea in rats: properties and potential. *Invest Ophthalmol Vis Sci* 2013; **54**(5): 3224-33.
16. Hos D, van Essen TH, Bock F, et al. [Decellularized collagen matrix from tilapia fish scales for corneal reconstruction (BioCornea)]. *Ophthalmologe* 2014; **111**(11): 1027-32.
17. van Essen TH, van Zijl L, Possemiers T, et al. Biocompatibility of a fish scale-derived artificial cornea: Cytotoxicity, cellular adhesion and phenotype, and in vivo immunogenicity. *Biomaterials* 2016; **81**: 36-45.
18. Kawai K, Tsuno NH, Matsuhashi M, et al. CD11b-mediated migratory property of peripheral blood B cells. *J Allergy Clin Immunol* 2005; **116**(1): 192-7.
19. Fagerholm P, Lagali NS, Ong JA, et al. Stable corneal regeneration four years after implantation of a cell-free recombinant human collagen scaffold. *Biomaterials* 2014; **35**(8): 2420-7.

20. Hos D, Le VNH, Hellmich M, et al. Risk of Corneal Graft Rejection After High-risk Keratoplasty Following Fine-needle Vessel Coagulation of Corneal Neovascularization Combined With Bevacizumab: A Pilot Study. *Transplant Direct* 2019; **5**(5): e452.
21. Hos D, Schlereth S, Schrittenlocher S, et al. [Descemet membrane endothelial keratoplasty (DMEK) for graft failure after penetrating keratoplasty and in vascularized high-risk eyes]. *Ophthalmologe* 2021; **118**(6): 536-43.
22. Cursiefen C, Schaub F, Bachmann BO. [Update Minimally Invasive Lamellar Keratoplasty: DMEK, DSAEK and DALK]. *Klin Monbl Augenheilkd* 2016; **233**(9): 1033-42.
23. Chen SC, Telinius N, Lin HT, et al. Use of Fish Scale-Derived BioCornea to Seal Full-Thickness Corneal Perforations in Pig Models. *PLoS One* 2015; **10**(11): e0143511.
24. Stamate AC, Tataru CP, Zemba M. Emergency penetrating keratoplasty in corneal perforations. *Rom J Ophthalmol* 2018; **62**(4): 253-9.
25. Bock F, Cursiefen C. [Anti(lymph)angiogenic Strategies to Improve Corneal Graft Survival]. *Klin Monbl Augenheilkd* 2017; **234**(5): 674-8.
26. Hanada K, Igarashi S, Muramatsu O, Yoshida A. Therapeutic keratoplasty for corneal perforation: clinical results and complications. *Cornea* 2008; **27**(2): 156-60.
27. Jhanji V, Young AL, Mehta JS, Sharma N, Agarwal T, Vajpayee RB. Management of corneal perforation. *Surv Ophthalmol* 2011; **56**(6): 522-38.
28. Stamate AC, Tataru CP, Zemba M. Update on surgical management of corneal ulceration and perforation. *Rom J Ophthalmol* 2019; **63**(2): 166-73.
29. Maier P, Bohringer D, Reinhard T. Clear graft survival and immune reactions following emergency keratoplasty. *Graefes Arch Clin Exp Ophthalmol* 2007; **245**(3): 351-9.
30. The collaborative corneal transplantation studies (CCTS). Effectiveness of histocompatibility matching in high-risk corneal transplantation. The Collaborative Corneal Transplantation Studies Research Group. *Arch Ophthalmol* 1992; **110**(10): 1392-403.
31. Jabbehdari S, Rafii AB, Yazdanpanah G, Hamrah P, Holland EJ, Djalilian AR. Update on the Management of High-Risk Penetrating Keratoplasty. *Curr Ophthalmol Rep* 2017; **5**(1): 38-48.
32. Mahabadi N, Czyz CN, Tariq M, Havens SJ. Corneal Graft Rejection. StatPearls. Treasure Island (FL); 2020.
33. Reis A, Birnbaum F, Reinhard T. [Systemic immunosuppressives after penetrating keratoplasty]. *Ophthalmologe* 2007; **104**(5): 373-80.
34. Borderie VM, Sandali O, Bullet J, Gaujoux T, Touzeau O, Laroche L. Long-term results of deep anterior lamellar versus penetrating keratoplasty. *Ophthalmology* 2012; **119**(2): 249-55.
35. Guilbert E, Bullet J, Sandali O, Basli E, Laroche L, Borderie VM. Long-term rejection incidence and reversibility after penetrating and lamellar keratoplasty. *Am J Ophthalmol* 2013; **155**(3): 560-9 e2.
36. Maddula S, Davis DK, Maddula S, Burrow MK, Ambati BK. Horizons in therapy for corneal angiogenesis. *Ophthalmology* 2011; **118**(3): 591-9.
37. Chong EM, Dana MR. Graft failure IV. Immunologic mechanisms of corneal transplant rejection. *Int Ophthalmol* 2008; **28**(3): 209-22.
38. Trufanov SV, Subbot AM, Malozhen SA, Salovarova EP, Krakhmaleva DA. [Risk factors, clinical presentations, prevention, and treatment of corneal graft rejection]. *Vestn Oftalmol* 2016; **132**(6): 108-16.
39. Yamagami S, Dana MR, Tsuru T. Draining lymph nodes play an essential role in alloimmunity generated in response to high-risk corneal transplantation. *Cornea* 2002; **21**(4): 405-9.
40. Bock F, Maruyama K, Regenfuss B, et al. Novel anti(lymph)angiogenic treatment strategies for corneal and ocular surface diseases. *Prog Retin Eye Res* 2013; **34**: 89-124.
41. Niederkorn JY. Mechanisms of corneal graft rejection: the sixth annual Thygeson Lecture, presented at the Ocular Microbiology and Immunology Group meeting, October 21, 2000. *Cornea* 2001; **20**(7): 675-9.

42. Qazi Y, Hamrah P. Corneal Allograft Rejection: Immunopathogenesis to Therapeutics. *J Clin Cell Immunol* 2013; **2013**(Suppl 9).
43. Oh JY, Lee HJ, Ko AY, Ko JH, Kim MK, Wee WR. Analysis of macrophage phenotype in rejected corneal allografts. *Invest Ophthalmol Vis Sci* 2013; **54**(12): 7779-84.
44. Hamrah P, Dana MR. Corneal antigen-presenting cells. *Chem Immunol Allergy* 2007; **92**: 58-70.
45. Liu Y, Hamrah P, Zhang Q, Taylor AW, Dana MR. Draining lymph nodes of corneal transplant hosts exhibit evidence for donor major histocompatibility complex (MHC) class II-positive dendritic cells derived from MHC class II-negative grafts. *J Exp Med* 2002; **195**(2): 259-68.
46. Streilein JW. Immunological non-responsiveness and acquisition of tolerance in relation to immune privilege in the eye. *Eye (Lond)* 1995; **9 (Pt 2)**: 236-40.
47. Cursiefen C, Chen L, Saint-Geniez M, et al. Nonvascular VEGF receptor 3 expression by corneal epithelium maintains avascularity and vision. *Proc Natl Acad Sci U S A* 2006; **103**(30): 11405-10.
48. Hos D, Cursiefen C. Lymphatic vessels in the development of tissue and organ rejection. *Adv Anat Embryol Cell Biol* 2014; **214**: 119-41.
49. Regenfuss B, Bock F, Bachmann B, et al. [Topical inhibition of angiogenesis at the cornea. Safety and efficacy]. *Ophthalmologe* 2009; **106**(5): 399-406.
50. Hossain P, Tourkmani AK, Kazakos D, et al. Emergency corneal grafting in the UK: a 6-year analysis of the UK Transplant Registry. *Br J Ophthalmol* 2018; **102**(1): 26-30.

8. APPENDIX

8.1. Figures

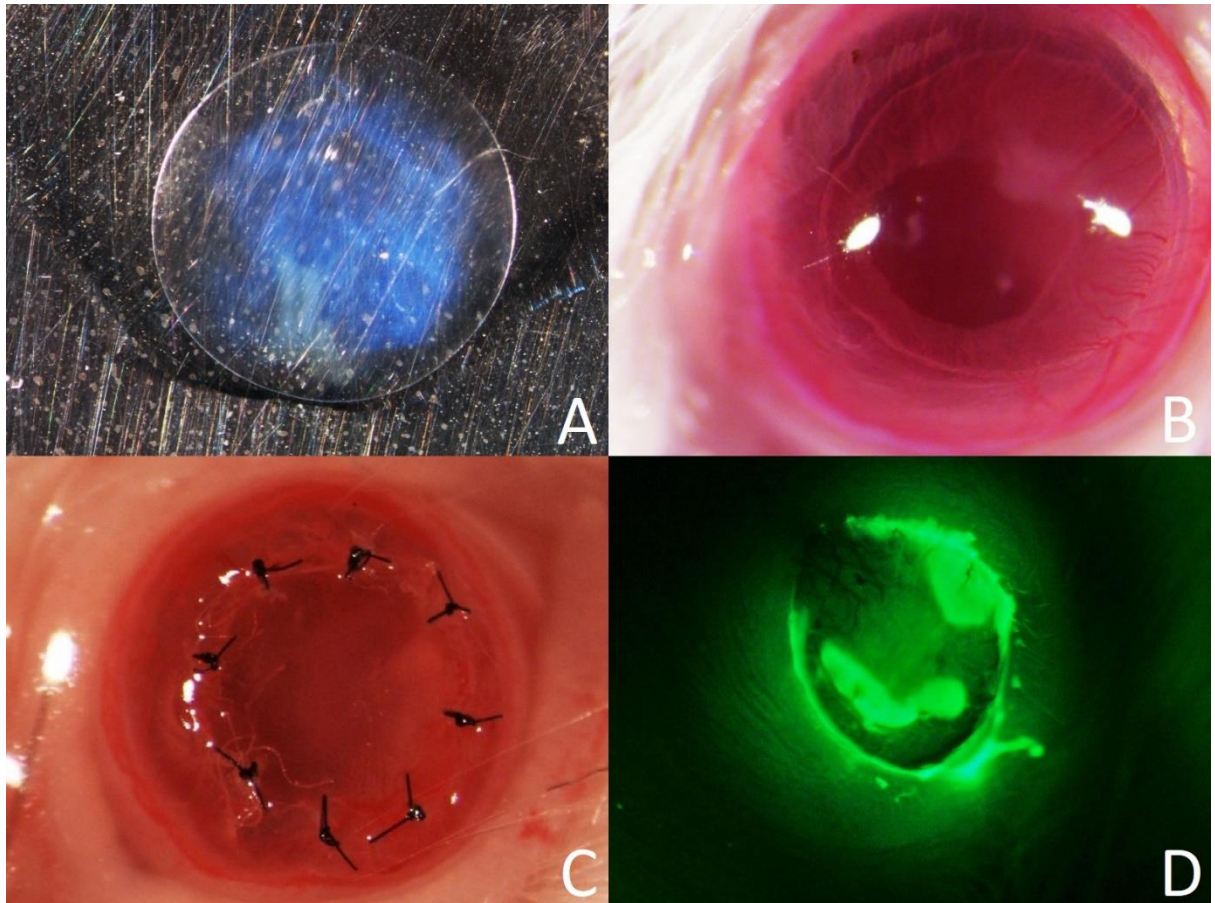


Figure 1. Keratoplasty with the FSCM and control allograft. Image A depicts a ready-for-transplantation FSCM-graft. Image B and C were taken during the keratoplasty process, before and after FSCM-graft transplantation. Image D depicts an implanted FSCM, one week after keratoplasty, showing partial epithelialization.

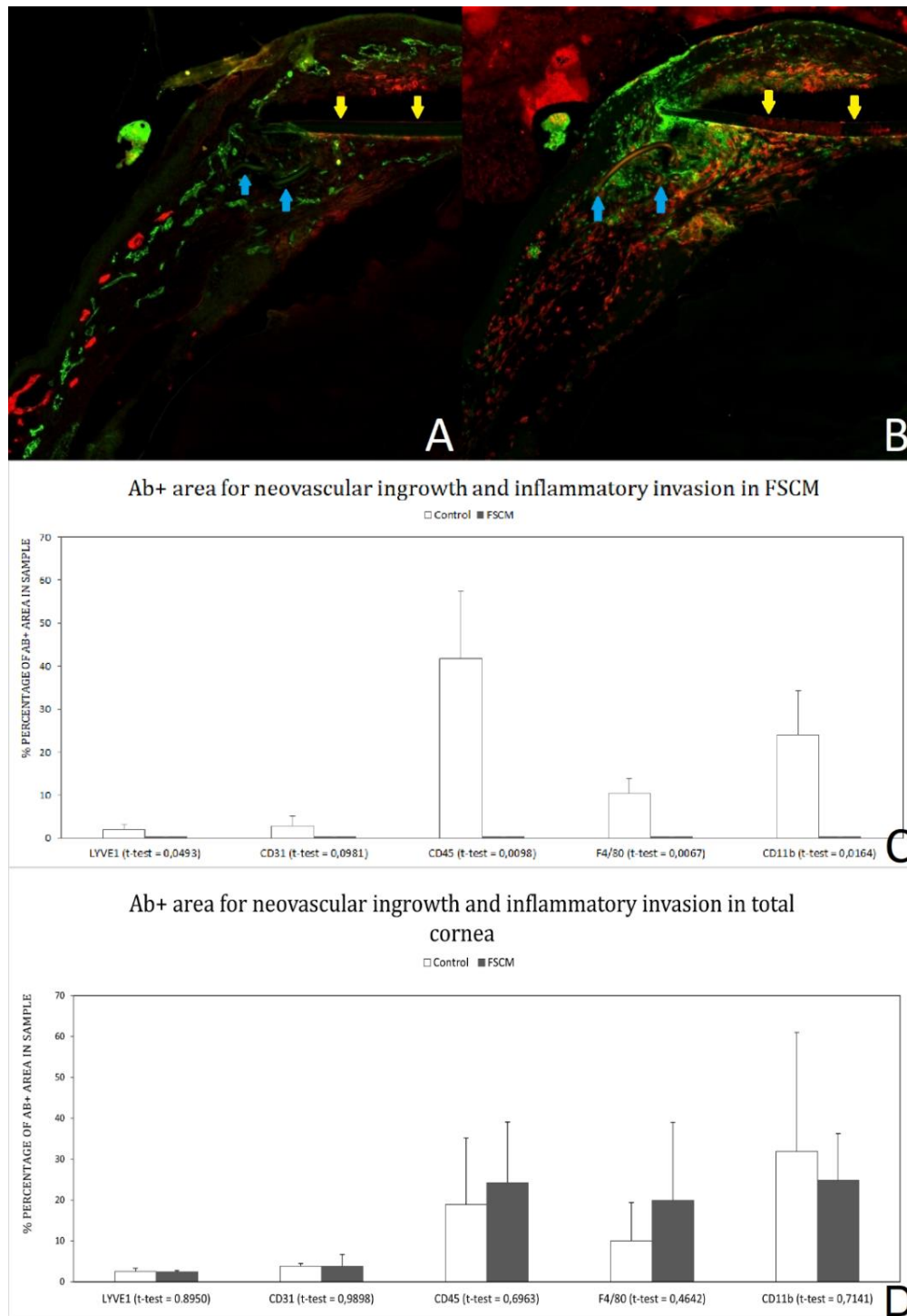


Figure 2. Immunohistochemical staining of cryosections of a FSCM- implanted sample. Yellow arrows indicate position of FSCM. Blue arrows indicate sutures. Image A depicts a Lyve1 (red) and CD31 (green) staining. Image B depicts a F4/80 (red) and CD11b (green) staining of the same sample. Of note is the higher concentration of inflammatory cells in the area around sutures. Chart C depicts the percentage of antibody-positive area for the LYVE1, CD31, CD45, F4/80 and CD11b markers in the FSCM (allogenic corneal transplant for the control group). For purposes of understanding, a dark gray line was painted manually to indicate 0% antibody-positive area for all tested markers in the FSCM group. Chart D depicts the percentage of antibody-positive area for the same markers in the recipient cornea.

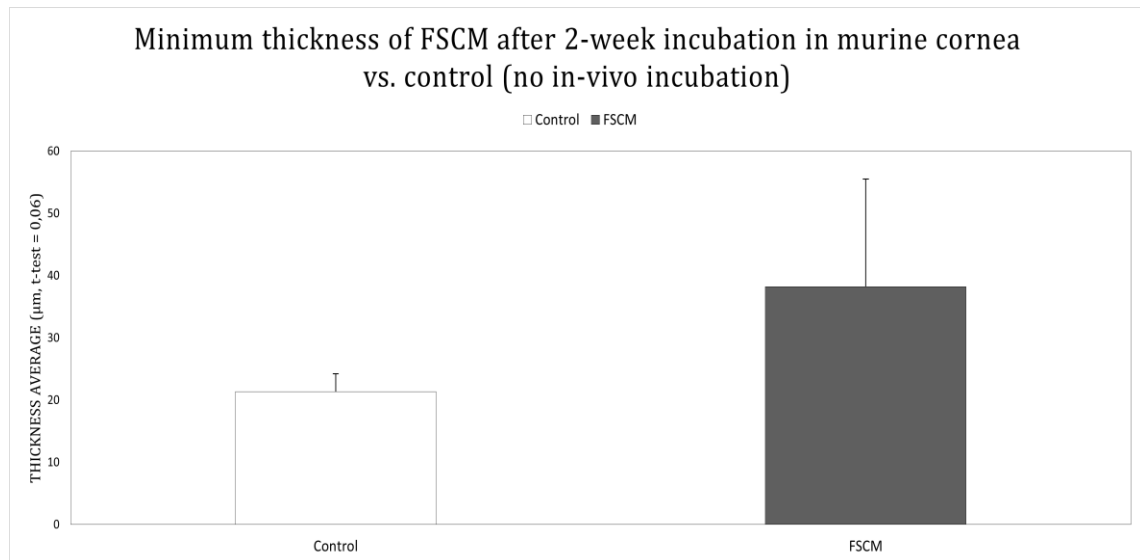


Figure 3. Minimum thickness of implanted FSCM after a 2-week period of incubation in murine cornea compared to minimum thickness of not-implanted FSCM having undergone the same histological preparation procedure (control). The measurements were performed with help from the image analyzing program Cell[^]F.

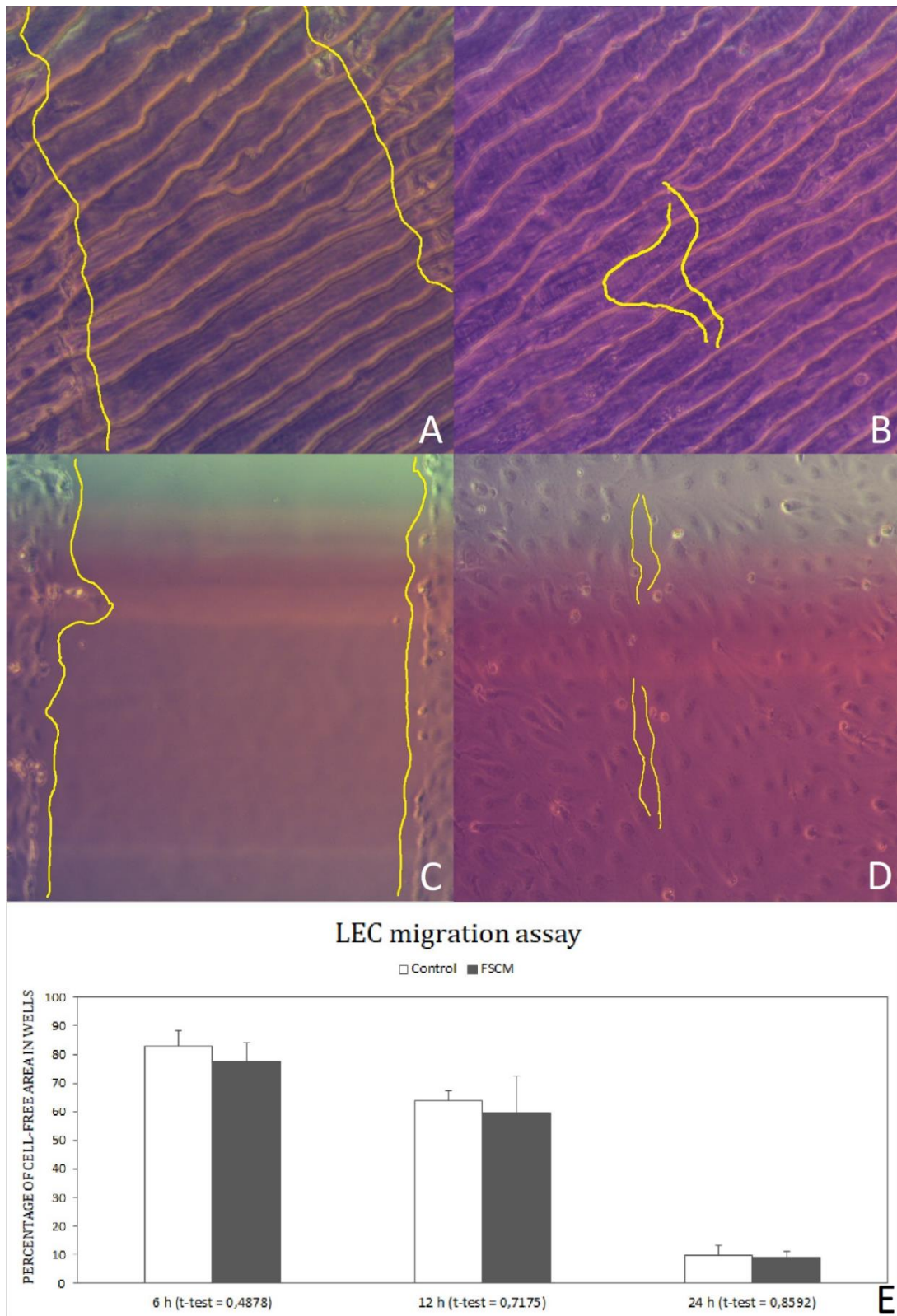


Figure 4: LEC migration on the FSCM. A and B depict the FSCM scratch-area (A and B) and control-well scratch-area (C and D) at timepoints 0 and 24. The chart (E) depicts the percentage of FSCM- area free of LECs at time points 0, 6, 12 and 24 h since start of migration assay.

8.2. Tables

Table 1. Percentage of antibody-positive area inside the FSCM (allogenic corneal transplant for the control group) (F = FSCM Group, C = Control Group).

Percentage of Antibody- positive Area in Graft					
Sample	Lyve1	CD31	CD45	F4/80	CD11 b
F1	0	0	0	0	0
F2	0	0	0	0	0
F3	0	0	0	0	0
C1	0.69	5.37	37.55	12.6	16.56
C2	3.09	2.09	28.69	12.14	35.89
C3	2.04	1	59.09	6.35	19.44
FSCM Group Average	0	0	0	0	0
Control Group Average	1.94	2.82	41.78	10.36	23.96
FSCM Group STDV	0	0	0	0	0
Control Group STDV	1.2	2.27	15.63	3.48	10.43
P-Value	0.049	0.098	0.01	0.007	0.016

Table 2. Percentage of antibody-positive area in recipient tissue 2 weeks after FSCM implantation (allogenic corneal transplant for the control group) (F = FSCM Group, C = Control Group).

Percentage of Antibody- positive Area in Recipient Tissue					
Sample	Lyve1	CD31	CD4 5	F4/80	CD11 b
F1	2.69	7.03	38.19	41.92	12.72
F2	2.45	1.60	8.64	10	35.33
F3	2.12	2.84	25.81	7.85	26.41
C1	2.17	3.03	37.66	6.6	17.9
C2	3.44	4.1	10.14	20.6	12.48
C3	1.86	4.27	8.83	2.81	65.37
FSCM Group Average	2.42	3.82	24.21	19.92	24.82
Control Group Average	2.49	3.8	18.88	10	31.92
FSCM Group STDV	0.28	2.84	14.84	19.08	11.39
Control Group STDV	0.84	0.68	16.28	9.37	29.1
P-Value	0.895	0.99	0.696	0.464	0.714

Table 3. Minimum thickness of FSCM after 2-week incubation in murine cornea vs. control (no *in vivo* incubation) (F = FSCM Group, C = Control Group).

Sample	Minimum Thickness of FSCM (µm)
F1	42.59
F2	19.19
F3	52.95
C1	28.99
C2	18.11
C3	20.4
C4	25.93
C5	21.93
Incubated FSCM Group Average	38.24
Control Group Average	21.35
Incubated FSCM Group STDV	17.29
Control Group STDV	2.9
P-Value	0.06

Table 4. Percentage of FSCM- area free of lymphatic endothelial cells at time points 0, 6, 12 and 24 h (F = FSCM Group, C = Control Group).

Percentage of Cell-free Area in Measured Timepoints				
Wells	0 h	6 h	12 h	24 h
F1	100	87.72	82.06	5.29
F2	100	65.22	59.28	11.69
F3	100	79.9	37.22	10.13
C1	100	95.19	71.07	12.49
C2	100	79.53	58.88	2.8
C3	100	80.07	63.4	14.09
FSCM Group Average	100	77.61	59.52	9.04
Control Group Average	100	83.1	63.83	9.8
FSCM Group STDV		11.42	22.42	3.34
Control Group STDV		8.13	5.18	6.11
p-value		0.488	0.717	0.859